



Distributed Control of DC Microgrids for Optimal Coordination of Conventional and Renewable Generators

Fan, Zhen; Fan, Bo; Liu, Wenxin

Published in:
IEEE Transactions on Smart Grid

DOI (link to publication from Publisher):
[10.1109/TSG.2021.3094878](https://doi.org/10.1109/TSG.2021.3094878)

Publication date:
2021

Document Version
Accepted author manuscript, peer reviewed version

[Link to publication from Aalborg University](#)

Citation for published version (APA):
Fan, Z., Fan, B., & Liu, W. (2021). Distributed Control of DC Microgrids for Optimal Coordination of Conventional and Renewable Generators. *IEEE Transactions on Smart Grid*, 12(6), 4607-4615.
<https://doi.org/10.1109/TSG.2021.3094878>

General rights

Copyright and moral rights for the publications made accessible in the public portal are retained by the authors and/or other copyright owners and it is a condition of accessing publications that users recognise and abide by the legal requirements associated with these rights.

- Users may download and print one copy of any publication from the public portal for the purpose of private study or research.
- You may not further distribute the material or use it for any profit-making activity or commercial gain
- You may freely distribute the URL identifying the publication in the public portal -

Take down policy

If you believe that this document breaches copyright please contact us at vbn@aub.aau.dk providing details, and we will remove access to the work immediately and investigate your claim.

Distributed Control of DC Microgrids for Optimal Coordination of Conventional and Renewable Generators

Zhen Fan, *Graduate Student Member, IEEE*, Bo Fan, *Member, IEEE*, Wei Zhang, *Senior Member, IEEE*, Wenxin Liu, *Senior Member, IEEE*

Abstract—DC microgrids are increasing in popularity due to their simplicity and high energy efficiency, and becoming an appealing solution for the coordination of multiple conventional generators (CGs) and renewable generators (RGs). This article presents a distributed discrete-time control scheme to achieve the optimal coordination of CGs and RGs, where the generation cost of the CGs is minimized and the energy utilization of RGs is maximized. A certain degree of proportional load sharing among the RGs is also achieved to improve the stability margin and dynamic performance of dc microgrids. The designed control algorithm can maintain the bus voltages in their safe operating ranges. Besides, since the proposed control algorithm is developed in the discrete-time domain directly, it can avoid the possible instability impact of the digital implementation of control algorithms. Based on the Lyapunov analysis, the stability and convergence of the closed-loop system are analyzed rigorously. Finally, simulation results based on a detailed switch-level dc microgrid model illustrate the advantages of the proposed optimal control algorithm.

Index Terms—Optimal coordination, distributed discrete-time control, conventional and renewable generator, dc microgrid.

I. INTRODUCTION

A dc microgrid can be defined as a cluster of distributed generators (DGs) including the conventional and renewable ones, loads, and energy storage devices accumulated in the vicinity of each other [1]. Since dc microgrids do not have issues related to frequency synchronization and reactive power regulation, it is less technically challenging than designing control schemes in ac microgrids. Therefore, dc microgrids are growing in popularity, especially for some special high-performance applications, and becoming a quite appealing alternative for the coordination of multiple conventional generators (CGs) and renewable generators (RGs) [2].

In dc microgrids, generation cost minimization is one of the essential optimization objectives [3, 4]. In the past, many works have realized this objective in a centralized way [5-7], and their reliability, flexibility, and scalability have been improved

through distributed optimization schemes [8-10]. However, these optimization algorithms are applied separately with control at different time scales by obtaining the optimal operating points periodically for given conditions [11]. The consequence is that even slight disturbances such as load changes will trigger real-time control adjustments so that the operating points will not be optimal. To overcome this issue, optimization is preferable to be realized through real-time control methods.

In recent years, there appear a few studies that try to bridge the gap between periodic optimization and real-time control [12-16]. In [12], a distributed consensus algorithm is proposed to solve the generation cost optimization problem for a multiple-bus dc microgrid. In [13], the generation cost is optimized considering the RGs' maximum capacities. However, individual bus voltage regulation is not realized in [12, 13]. The bus voltages may become dangerously high or low during both the transient- and steady-state. To resolve this issue, Wang *et. al.* [14] proposed a unified distributed control strategy for dc microgrids with generation and individual bus voltage constraints. Nevertheless, plenty of information has to be exchanged among the distributed controllers so that high-bandwidth communication is needed. Moreover, although these designs [12-14] can respond to changing operating conditions, the closed-loop system stability analysis is not provided [15]. For this problem, Peng *et. al.* [16] proposed a distributed optimal controller with guaranteed closed-loop system stability. However, this method is designed to minimize the generation cost which is originally utilized for CGs. The coordination requirements of multiple CGs and RGs are not well addressed.

In tradition, the costs of RGs are considered as the initial installation and subsequent maintenance costs. Hence, RGs are usually encouraged to work at maximum peak power tracking (MPPT) mode to bring a higher return on investment. When their maximum generation capacities of RGs are lower than the load demand, CGs are applied to ensure the supply-demand balance with optimized generation cost. When the RGs'

Manuscript received November 23, 2020; revised May 12, 2021; accepted June 25, 2021. This work was supported by the U.S. Office of Naval Research under Grant N00014-21-1-2175. Paper no. TSG-01757-2020. (*Corresponding author: Bo Fan.*)

Z. Fan, W. Zhang, and W. Liu are with the Smart Microgrid and Renewable Technology (SMRT) Research Laboratory, Department of Electrical and

Computer Engineering, Lehigh University, Bethlehem, PA 18015, USA (email: zhf217@lehigh.edu; wex221@lehigh.edu; wliu@lehigh.edu).

Bo Fan is with the Department of Energy Technology, Aalborg University, Aalborg 9220, Denmark (e-mail: bof@et.aau.dk).

maximum generation capacities are more than demand, they cannot operate at the MPPT mode. Instead, proportional load sharing among the RGs is usually considered to improve the stability margin and dynamic performance of dc microgrids [17, 18]. Therefore, it is necessary to design distributed control strategies to achieve the optimal coordination of multiple CGs and RGs in dc microgrids, i.e., CGs' generation cost minimization and RGs' energy utilization maximization with proportional load sharing among them.

Furthermore, from the perspective of sampling, most of the control schemes introduced above are developed in the continuous-time domain. Whereas, in modern control systems, most system-level control strategies are implemented with digital controllers and communication systems. These controllers and communication systems are intrinsically discrete-time [17, 19], where signal sampling, control signal update, and data transmission only happen at discrete-time instants. However, the discrete-time implementation of continuous-time-based controls may cause the instability of the closed-loop system [20]. To avoid the instability impact, control schemes are preferred to be directly designed and analyzed in the discrete-time domain.

This article presents a distributed control scheme for dc microgrids to achieve the optimal coordination of CGs and RGs. The main contributions of this article are summarized as :

- 1) The presented control method is directly developed in the discrete-time domain. The possible instability of the discrete-time implementation of control algorithms is avoided;
- 2) With the proposed control scheme, the generation cost of CGs is minimized and the energy utilization of RGs is maximized. Besides, a certain degree of proportional load sharing among the RGs is achieved, simultaneously;
- 3) The bus voltages are guaranteed to be within their safe operating ranges during both the transient- and steady-state. The system reliability is improved;
- 4) The closed-loop system stability and convergence are analyzed theoretically via the Lyapunov synthesis. The bus voltages and output currents can converge to their optimal operating points asymptotically.

The rest of this article is organized as follows: Section II illustrates the model of the considered dc microgrid. In Section III, the convex optimization problem with constraints is introduced. Afterward, the distributed discrete-time optimal coordination control algorithm is developed in Section IV. In Section V, simulation results are offered to showcase the merits of the proposed algorithms. Lastly, the conclusion and further studies are discussed in Section VI.

II. DC MICROGRID MODELING

Fig. 1. presents the model of a dc microgrid composed of an electrical network (solid line) and a communication network (dashed line). The former is a physical grid for delivering electric power from DGs to loads, while the latter is a sparse network for information sharing among the DGs' distributed controllers. The energy source is connected to the electrical network through a dc/dc converter (e.g., photovoltaic panels and fuel cells) or an ac/dc one (e.g., diesel generators) [13].

Since the distribution lines are predominantly resistive in dc microgrids, the dynamic effects of the line inductance and capacitance are neglected for simplicity [17, 18].

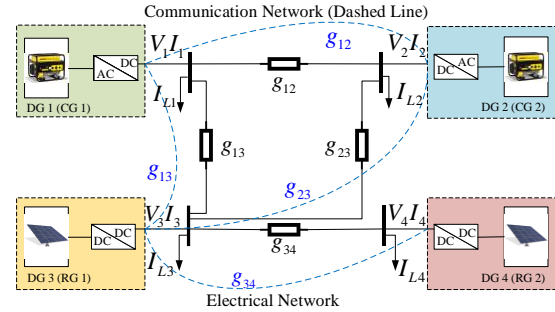


Fig. 1. Model of a dc microgrid.

A. Electrical Network Modeling

The electrical network model of a dc microgrid can be treated as an undirected and connected graph $\mathcal{G}_E = (\mathcal{V}_E, \mathcal{E}_E)$, where the set $\mathcal{V}_E = \mathcal{V}_{CG} \cup \mathcal{V}_{RG}$ with \mathcal{V}_{CG} representing the buses with CGs and \mathcal{V}_{RG} representing the buses with RGs, and the set $\mathcal{E}_E \subseteq \mathcal{V}_E \times \mathcal{V}_E$ denotes the distribution lines. The nodal admittance matrix is then defined as $\mathbf{G} = \{G_{ij}\} \in \mathbb{R}^{n \times n}$ with n being the number of buses. $G_{ij} \in \mathbb{R}$ is given as

$$G_{ij} = \begin{cases} \sum_{m=1, m \neq i}^n g_{im}, & i = j \\ -g_{ij}, & i \neq j \end{cases}$$

where $g_{ij} = g_{ji} \in \mathbb{R}^+$ is the conductance of the distribution line between bus i and bus j if $(i, j) \in \mathcal{E}_E$, and $g_{ij} = g_{ji} = 0$ otherwise. Notice that \mathbf{G} is also the Laplacian matrix of graph \mathcal{G}_E . Next, according to Kirchhoff's Current Laws, one has

$$I_i = \sum_{j=1}^n g_{ij}(V_i - V_j) + I_{L_i} = \sum_{j=1}^n G_{ij}V_j + I_{L_i}, i \in \mathcal{V}_E \quad (1)$$

where $I_i \in \mathbb{R}$ denotes the output current of DG i , and $V_i \in \mathbb{R}$, $I_{L_i} \in \mathbb{R}$ denote the voltage and load current of bus i , respectively. Next, rewriting (1) in a compact form yields

$$\mathbf{I} = \mathbf{G}\mathbf{V} + \mathbf{I}_L \quad (2)$$

where $\mathbf{V} = [V_1, V_2, \dots, V_n]^T \in \mathbb{R}^n$, $\mathbf{I}_L = [I_{L_1}, I_{L_2}, \dots, I_{L_n}]^T \in \mathbb{R}^n$, and $\mathbf{I} = [I_1, I_2, \dots, I_n]^T \in \mathbb{R}^n$. In this study, a system-level coordination method for DGs including CGs and RGs is developed. For simplicity, the impact of the CGs' inertia is neglected [13, 16]. In (2), \mathbf{V} is treated as the control signal by assuming that the bus voltage reference can be achieved accurately and quickly by each DG's voltage control loop.

B. Communication Network Modeling

As illustrated in Fig. 1, the communication network among the DGs' controllers can be considered as an undirected and connected graph $\mathcal{G}_C = (\mathcal{V}_C, \mathcal{E}_C)$, with the set $\mathcal{V}_C = \{1, 2, \dots, n\}$ denoting the n distributed controllers and the set $\mathcal{E}_C \subseteq \mathcal{V}_C \times \mathcal{V}_C$ denoting the communication links among the controllers [21]. In this study, the communication network is designed identically to the electrical one, i.e., $\mathcal{G}_C = \mathcal{G}_E$ as shown in Fig.1. Hence, the Laplacian matrix of graph \mathcal{G}_C is also identical to the nodal admittance matrix \mathbf{G} .

III. OPTIMAL CONTROL PROBLEM FORMULATION

This section introduces the considered optimal coordination problem of dc microgrids with multiple CGs and RGs.

In a dc microgrid, the generation costs of CGs can be represented by quadratic functions of their power outputs $P_i \in \mathbb{R}$, $i \in \mathcal{V}_{CG}$, which are expressed as [16]

$$f_i(P_i) = a_i P_i^2 + b_i P_i + c_i, i \in \mathcal{V}_{CG} \quad (3)$$

where $a_i, b_i, c_i \in \mathbb{R}^+$, $i \in \mathcal{V}_{CG}$, are the cost coefficients.

For RGs, their energy utilization is encouraged to be as much as possible to bring a higher return on investment due to their almost zero production cost. Also, the RGs are usually required to achieve the proportional load sharing objective to increase their control stability margins. Based on these requirements, the RGs' cost functions can be expressed as [13]

$$f_i(P_i) = \frac{(P_i - \bar{P}_i)^2}{\bar{P}_i} = \frac{1}{\bar{P}_i} P_i^2 - 2P_i + \bar{P}_i, i \in \mathcal{V}_{RG} \quad (4)$$

where $\bar{P}_i \in \mathbb{R}^+$, $i \in \mathcal{V}_{RG}$ are the maximum generation capacities of the RGs. $f_i(P_i)$ is minimized when the RG takes full advantage of its capacity. Therefore, RGs' energy maximization is inherently achieved, provided that cost minimization can be guaranteed. By introducing $a_i = 1/\bar{P}_i$, $b_i = -2$, $c_i = \bar{P}_i$, $i \in \mathcal{V}_{RG}$, the RG's cost function takes the same form as that for a CG in (3).

Because of the nonlinear relationship between P_i and V_i , the designs for power controllers are usually much more complex than those of the current ones [18]. Consider the fact that bus voltages in actual dc microgrids are usually close to 1 per unit (p.u.) during normal operation. To derive simple yet effective control designs, P_i (in p.u.) is approximated by I_i (in p.u.) with acceptable accuracy according to $P_i = V_i I_i \approx I_i$ in the following analysis to strike a balance between control accuracy and practicality [16, 22]. By approximating P_i by I_i , the DGs' cost functions become

$$f_i(P_i) \approx f_i(I_i) = a_i I_i^2 + b_i I_i + c_i, i \in \mathcal{V}_E \quad (5)$$

where $a_i = 1/\bar{I}_i$, $b_i = -2$, $c_i = \bar{I}_i$ for $i \in \mathcal{V}_{RG}$ with $\bar{I}_i \in \mathbb{R}^+$ being the generation capacity of the RG.

A. Convex Optimization Problem Formulation

Consider the following convex optimization problem:

$$\begin{aligned} \min_{\mathbf{I}, \mathbf{V}} f(\mathbf{I}) &= \sum_{i=1}^n f_i(I_i) \\ \text{s. t.} \quad (2) & \\ \underline{V}_i \leq V_i \leq \bar{V}_i, i \in \mathcal{V}_{CG} & \\ 0 \leq I_i \leq \bar{I}_i, i \in \mathcal{V}_{RG} & \\ \underline{V}_i \leq V_i \leq \bar{V}_i, i \in \mathcal{V}_E & \end{aligned} \quad (6)$$

where $f(\cdot): \mathbb{R}^n \rightarrow \mathbb{R}$ denotes the total cost, $\underline{V}_i, \bar{V}_i \in \mathbb{R}^+$ are voltage lower and upper bounds of bus i , $i \in \mathcal{V}_E$, respectively, which are formulated to endure the secure operation of dc microgrids. $\underline{I}_i, \bar{I}_i \in \mathbb{R}$, $i \in \mathcal{V}_{CG}$, are the CGs' output current lower and upper bounds determined by the CGs' capacities.

Assumption 1: Slater's constraint qualification condition holds, i.e., there exists an interior point $\bar{\mathbf{V}} \in \Omega_V$, $\bar{\mathbf{I}} \in \Omega_I$, such that $\bar{\mathbf{I}} = \mathbf{G}\bar{\mathbf{V}} + \mathbf{I}_L$, where $\Omega_V = \{\mathbf{V} \in \mathbb{R}^n | \underline{V}_i \leq V_i \leq \bar{V}_i, i \in \mathcal{V}_E\}$, $\Omega_I = \{\mathbf{I} \in \mathbb{R}^n | \underline{I}_i \leq I_i \leq \bar{I}_i, i \in \mathcal{V}_{CG} \text{ and } 0 \leq I_i \leq \bar{I}_i, i \in \mathcal{V}_{RG}\}$.

Remark 1 (Convexity analysis): Notice that Ω_V and Ω_I are all convex sets. The equality constraint (2) is affine. Because

$\nabla^2 f = \text{diag}\{2a_1, 2a_2, \dots, 2a_n\} > 0$, the cost function $f(\mathbf{I})$ is also convex. Therefore, the optimization problem is convex.

B. Equivalent Optimality Condition

Before the development of the distributed optimal control strategy, an equivalent necessary and sufficient condition for the optimal solution to the convex optimization problem (6) is derived firstly. To begin with, the project operator is introduced. Let $\mathbf{P}_\Omega(\cdot): \mathbb{R}^n \rightarrow \Omega$ be a project operator expressed as $\mathbf{P}_\Omega(\mathbf{u}) = \arg \min_{\mathbf{v} \in \Omega} \|\mathbf{v} - \mathbf{u}\|$, where $\Omega \subseteq \mathbb{R}^n$ is a closed convex set.

Lemma 1 ([23]): The following inequality holds for the project operator $\mathbf{P}_\Omega(\cdot)$ and any closed convex set $\Omega \subseteq \mathbb{R}^n$:

$$(\mathbf{u} - \mathbf{P}_\Omega(\mathbf{u}))^T (\mathbf{P}_\Omega(\mathbf{u}) - \mathbf{v}) \geq 0, \forall \mathbf{u} \in \mathbb{R}^n, \mathbf{v} \in \Omega.$$

Under Assumption 1, the necessary and sufficient conditions for the optimal solutions of (6) are given as follows.

Lemma 2 ([24]): $\mathbf{V}^* \in \mathbb{R}^n$, $\mathbf{I}^* \in \mathbb{R}^n$ is the optimal solution to (6) if and only if there exist $\mathbf{y}^* \in \mathbb{R}^n$ such that

$$\begin{cases} \mathbf{V}^* - \mathbf{P}_{\Omega_V}(\mathbf{V}^* + \alpha \mathbf{G}\mathbf{y}^*) = \mathbf{0} \\ \mathbf{I}^* - \mathbf{P}_{\Omega_I}[\mathbf{I}^* - \alpha(\boldsymbol{\mu}^* + \mathbf{y}^*)] = \mathbf{0} \\ \mathbf{I}^* - \mathbf{G}\mathbf{V}^* - \mathbf{I}_L = \mathbf{0} \end{cases} \quad (7)$$

where $\alpha \in \mathbb{R}^+$ is a user-defined step size, and $\boldsymbol{\mu}^* = [\mu_1^*, \mu_2^*, \dots, \mu_n^*]^T \in \mathbb{R}^n$ with

$$\mu_i^* = \left. \frac{\partial f_i}{\partial I_i} \right|_{I_i=I_i^*} = 2a_i I_i^* + b_i, i \in \mathcal{V}_E.$$

IV. DISTRIBUTED DISCRETE-TIME OPTIMAL CONTROL

Consider that the distributed controllers are implemented by digital controllers and update only at periodic discrete-time instants $t = kT$, $k \in \mathbb{N}$. Denote $(\cdot)_{ik} = (\cdot)_i(kT)$, $i \in \mathcal{V}_E$. According to (7), for DG i , $i \in \mathcal{V}_E$, the control algorithm for solving the optimization problem (6) is proposed as

$$V_{i(k+1)} = \mathbf{P}_{\Omega_{V_i}}[V_{ik} + \alpha \sum_{j=1}^n g_{ij} ((y_{ik} + \hat{I}_{ik} - I_{ik}) - (y_{jk} + \hat{I}_{jk} - I_{jk}))] \quad (8)$$

$$\hat{I}_{i(k+1)} = \mathbf{P}_{\Omega_{I_i}}[\hat{I}_{ik} - \alpha(\mu_{ik} + y_{ik} + \hat{I}_{ik} - I_{ik})] \quad (9)$$

$$y_{ik} = y_{i(k-1)} + \hat{I}_{ik} - I_{ik} \quad (10)$$

where $\Omega_{V_i} = \{V_i \in \mathbb{R} | \underline{V}_i \leq V_i \leq \bar{V}_i\}$, $i \in \mathcal{V}_E$, $\Omega_{I_i} = \{I_i \in \mathbb{R} | \underline{I}_i \leq I_i \leq \bar{I}_i\}$, $i \in \mathcal{V}_{CG}$ and $\Omega_{I_i} = \{I_i \in \mathbb{R} | 0 \leq I_i \leq \bar{I}_i\}$, $i \in \mathcal{V}_{RG}$, $\hat{I}_{ik} \in \mathbb{R}$ is the internal current control signal, $y_{ik} \in \mathbb{R}$ is an auxiliary variable, and $\mu_{ik} = 2a_i \hat{I}_{ik} + b_i$, $i \in \mathcal{V}_E$.

The control diagram is given in Fig. 2. For DG i only the lumped variable $y_{ik} + \hat{I}_{ik} - I_{ik}$ is required to be transmitted to its neighbors. The exchanged information is limited. Moreover, as illustrated in Section II, g_{ij} is not zero if and only if DG i and DG j are connected through a physical distribution line. Therefore, the proposed algorithm (8)-(10) is distributed in the sense that each DG's local controller only requires its local information and the information from its neighbors.

Next, the stability and convergence results of the proposed controller (8)-(10) are demonstrated in the following theorem.

Theorem 1: Considering a dc microgrid modeled by (2) and the control algorithms are designed in (8)-(10), then the voltage \mathbf{V}_k and current \mathbf{I}_k can converge to an optimal solution of the optimization problem (6) if $\alpha \leq 1/\lambda_{max}(\mathbf{H})$, where λ_{max} is the maximum eigenvalue of \mathbf{H} expressed as

$$\mathbf{H} = \begin{bmatrix} \mathbf{G}^2 & -\mathbf{G} \\ -\mathbf{G} & (1 + 2\sigma)\mathbb{I}_n \end{bmatrix} \in \mathbb{R}^{2n \times 2n}$$

with $\sigma \geq 2 \max_i a_i \in \mathbb{R}^+$ is a constant, and $\mathbb{I}_n \in \mathbb{R}^{n \times n}$ is the identity matrix.

Proof: Please see Appendix.

For converters, since the bus voltages and output currents are strictly governed by (2), only the bus voltages can be independently controlled, whose constraints in (6) can be ensured through the project operator as designed in (8). However, the constraints on the output currents cannot be guaranteed directly through the project operator due to the relationship between bus voltages and output currents. Hence, an internal current control signal \hat{I}_{ik} is introduced to facilitate the regulation of DGs' output currents to ensure their steady-state values satisfy (6).

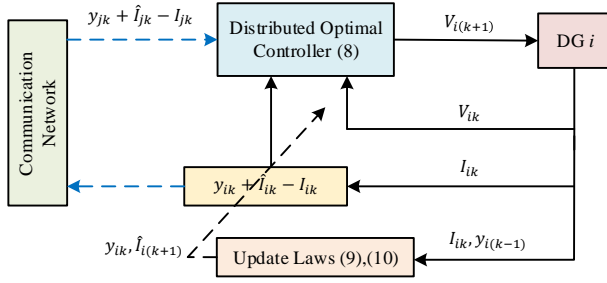


Fig. 2. Diagram of the proposed control algorithm for DG i .

TABLE I
SYSTEM PARAMETERS

Quantity	Value
Line conductance $g_{12}, g_{13}, g_{23}, g_{34}$ (p.u.)	4.608
Current upper bounds of CGs \bar{I}_1, \bar{I}_2 (p.u.)	1.0
Current lower bounds of CGs $\underline{I}_1, \underline{I}_2$ (p.u.)	0.0
Voltage upper bounds $\bar{V}_1, \bar{V}_2, \bar{V}_3, \bar{V}_4$ (p.u.)	1.05
Voltage lower bounds $\underline{V}_1, \underline{V}_2, \underline{V}_3, \underline{V}_4$ (p.u.)	0.95
Cost coefficients of CG 1 a_1, b_1, c_1 (p.u.)	0.1085 0.0832 0.008
Cost coefficients of CG 2 a_2, b_2, c_2 (p.u.)	0.1085 0.0260 0.006
Filter capacitance (μF)	250, 200, 250, 250
Filter inductance (mH)	2.0, 2.0, 1.5, 2.0
Filter resistance (Ω)	0.2, 0.1, 0.1, 0.2
Nominal bus voltage ($V, 1$ p.u.)	48
Nominal power rate ($W, 1$ p.u.)	1000
Switching frequency (kHz)	10
Sampling period T (ms)	0.1

V. SIMULATION STUDIES

A. Simulation Setup

To evaluate the effectiveness of the designed distributed optimal controller for dc microgrids, switch-level simulations are performed in MATLAB/Simulink. The topology of the dc microgrid is demonstrated in Fig. 1. Since all DGs are connected to the microgrid through converters, each DG is modeled as a buck converter connecting to the electrical network through an LC -filter. The system parameters are listed in Table I [15]. Based on Theorem 1, in the simulations, the maximum value of a_i is approximately 3.33 (Case II). Hence, σ is selected as 6.67. Afterward, one has $\lambda_{max} = 340.779$, so

$\alpha \leq 1/\lambda_{max}(\mathbf{H}) = 0.00293$. To allow for a stability margin, α is selected as 0.001.

B. Case I: Constant RG Capacities

In this case, the effectiveness of the proposed optimal controller is tested under the constant generation capacities of RGs which are all 1.0 p.u. and the load conditions listed in Table II. The results are delivered in Figs. 3-4.

From Fig. 3, one can see that the bounded bus voltage regulation is ensured during both the transient- and steady-state. The output currents of all CGs and RGs are presented in Fig. 4. Before 8 s, since the total capacity of RGs is sufficient for the loads, only RGs offer the power supply and the current outputs are shared equally. From 8 s to 12 s, when the maximum capacities for RGs are insufficient, the CGs cover the shortage and meet the total load demand.

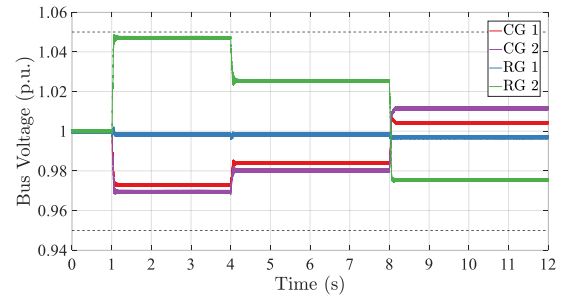


Fig. 3. Trajectories of bus voltages with constant RG capacities.

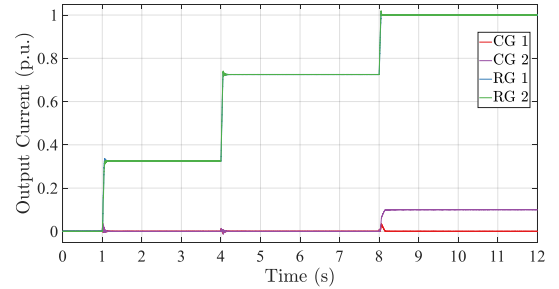


Fig. 4. Trajectories of output currents with constant RG capacities.

TABLE II
LOAD PROFILES IN CASES I, III, AND IV

Bus	0-1 s	1-4 s	4-8 s	8-12 s
1	0	0.10 p.u.	0.05 p.u.	0.0 p.u.
2	0	0.15 p.u.	0.10 p.u.	0.0 p.u.
3	0	0.30 p.u.	0.70 p.u.	1.0 p.u.
4	0	0.10 p.u.	0.60 p.u.	1.1 p.u.

TABLE III
COMPARISON OF $f(\mathbf{I})$ IN CASE I

Time	Proposed Method	Ground Truth	Relative Error
1-4 s	0.925256 p.u.	0.925250 p.u.	0.000648%
4-8 s	0.165252 p.u.	0.165250 p.u.	0.001210%
8-12 s	0.017685 p.u.	0.017685 p.u.	0.000000%

The optimality of the proposed method is demonstrated in Table III. The cost $f(\mathbf{I})$ of the proposed method is directly obtained from the simulation results. The ground truth of $f(\mathbf{I})$ is calculated through the convex optimization tool. As shown in

Table III, the relative errors between $f(\mathbf{I})$ of the proposed method and that of the ground truth are very close to zero. Therefore, the proposed method achieves the optimization goal.

C. Case II: Dynamic RG Capacities

In this case, the effectiveness of the proposed optimal controller is tested under dynamic RG capacities, which are formulated as piecewise linear functions [25]

$$\bar{I}_3 = \begin{cases} 1, & 0 \leq t < 2 \text{ s} \\ -0.175t + 1.35, & 2 \leq t \leq 6 \text{ s} \\ 0.125t - 0.45, & 6 \leq t \leq 10 \text{ s} \\ 0.8, & 10 \leq t \leq 12 \text{ s} \end{cases}$$

$$\bar{I}_4 = \begin{cases} 1, & 0 \leq t < 2 \text{ s} \\ -0.150t + 1.30, & 2 \leq t \leq 6 \text{ s} \\ 0.125t - 0.35, & 6 \leq t \leq 10 \text{ s} \\ 0.9, & 10 \leq t \leq 12 \text{ s} \end{cases}$$

where \bar{I}_3 and \bar{I}_4 are the capacities of RG 1 and RG 2, respectively. The load profile is listed in Table IV. The results are given in Figs. 5-9.

As demonstrated in Fig. 5, under the situation of dynamic RG capacities, all bus voltages are again ensured to be restricted in their security constraints. In Figs. 6-7, when the maximum capacities for RGs are insufficient, the CGs can cover the shortage and when they are sufficient, only RGs offer the loads. The RGs' utilization levels are given in Fig. 8. One can notice that the utilization levels of RGs are almost identical for all time, which means that proportional load sharing is achieved among RGs.

Bus	0-1 s	1-6.5 s	6.5-12 s
1	0	0.1 p.u.	0.1 p.u.
2	0	0.1 p.u.	0.1 p.u.
3	0	0.3 p.u.	0.7 p.u.
4	0	0.1 p.u.	0.6 p.u.

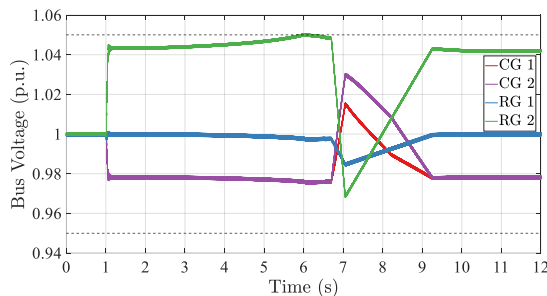


Fig. 5. Trajectories of bus voltages with dynamic RG capacities.

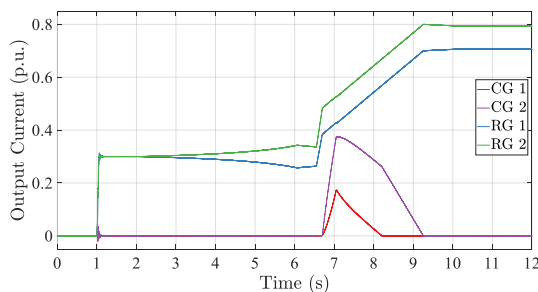


Fig. 6. Trajectories of output currents with dynamic RG capacities.

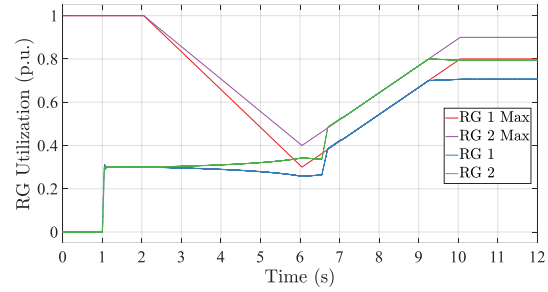


Fig. 7. Trajectories of RG utilization with dynamic RG capacities.

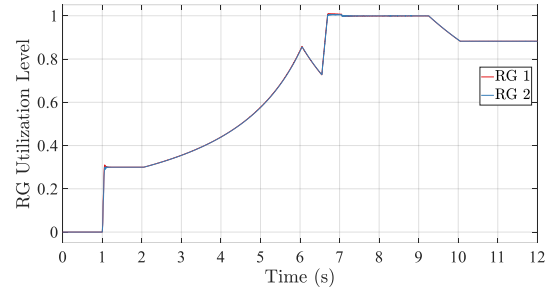


Fig. 8. Trajectories of RG utilization levels with dynamic RG capacities.

Moreover, to demonstrate the optimality of the proposed method, a dynamic relative error based on the optimal condition (7) is defined as

$$\text{Relative Error} = \begin{bmatrix} \mathbf{V} - \mathbf{P}_{\Omega_V}(\mathbf{V} + \alpha \mathbf{Gy}) \\ \mathbf{I} - \mathbf{P}_{\Omega_I}[\mathbf{I} - \alpha(\boldsymbol{\mu} + \mathbf{y})] \end{bmatrix}$$

Hence, the optimal control objective is achieved if the relative error is zero. In Fig. 9, one can notice that the relative errors are very close to zero. The short transience shows that the proposed controller can quickly drive the system to the optimal operating point when loads and RGs' capacities change. Online optimization is thus achieved.

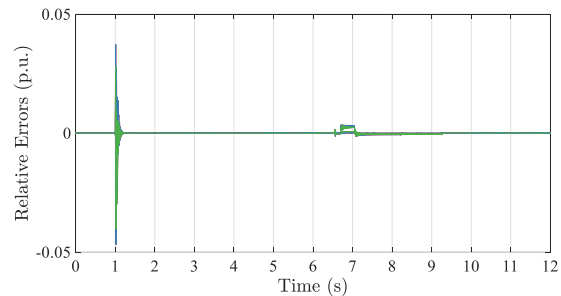


Fig. 9. Trajectories of relative errors with dynamic RG capacities.

D. Case III: Line Parameter Uncertainties

In this case, line parameter uncertainties ($\pm 5\%$) are considered to test the control performance of the proposed method. The generation capacities of RGs are 1.0 p.u. and the load conditions are listed in Table II. Figs. 10-11 show the simulation results.

From Fig. 10, it can be noticed that the bounded bus voltage regulation is again achieved during both the transient- and steady-state by taking the advantages of the project operator in (8). In Fig. 11, the trajectories of the DGs' output currents are

given, whose performance is similar to the results in Fig. 4 with accurate line parameters.

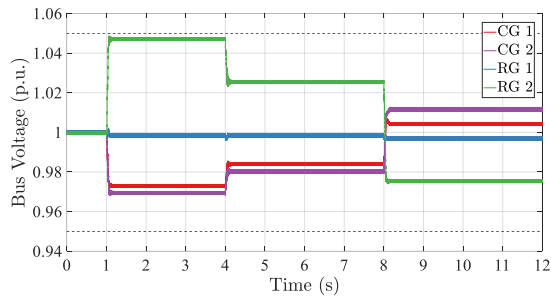


Fig. 10. Trajectories of bus voltages with line parameter uncertainties.

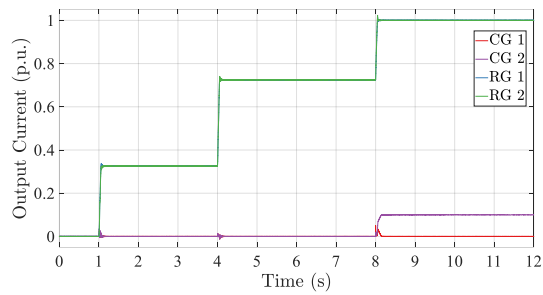


Fig. 11. Trajectories of output currents with line parameter uncertainties.

TABLE V
COMPARISON OF $f(\mathbf{I})$ IN CASE III

Time	Proposed Method	Ground Truth	Relative Error
1-4 s	0.925256 p.u.	0.925250 p.u.	0.000648%
4-8 s	0.165252 p.u.	0.165250 p.u.	0.001210%
8-12 s	0.017685 p.u.	0.017685 p.u.	0.000000%

Besides, the optimality of the proposed method in the presence of line parameter uncertainties is demonstrated in Table V. Interestingly, the resulted $f(\mathbf{I})$ values are the same as those in Table III with accurate line parameters. This is mainly because that the bus voltages as shown in Fig. 10 are always within their safe operating ranges. In such as case, the optimality condition (7) will be independent of the topology of the nodal admittance matrix \mathbf{G} , which is consistent with [13]. Therefore, online optimization is again achieved. However, if the optimal solution of the considered problem in (6) has one or more bus voltages staying at their boundaries, the proposed method may be unable to achieve the optimization objective in the presence of line parameter uncertainties.

E. Case IV: Communication Delay

In this case, the control performance is tested with constant communication delays. The dc microgrid is subject to the load condition in Table II. The corresponding results are given in Figs. 12-15.

The control performance of the proposed optimal controller with $500 \mu\text{s}$ communication delay is demonstrated in Figs. 12-13. It shows that the $500 \mu\text{s}$ communication delay does not have a significant impact on the performance of the proposed controller. Further, as shown in Figs. 14-15, a $1000 \mu\text{s}$ communication delay is added to the communication network. In this case, the controller can still guarantee the stability of the

system with oscillations. Based on these results, the proposed controller can withstand a $1000 \mu\text{s}$ communication delay or less.

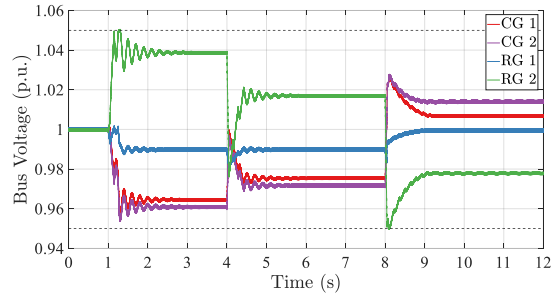


Fig. 12. Trajectories of bus voltages with $500 \mu\text{s}$ communication delay.

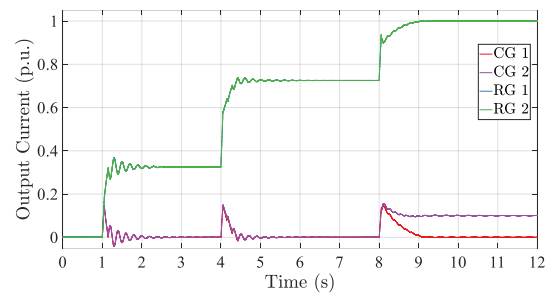


Fig. 13. Trajectories of output currents with $500 \mu\text{s}$ communication delay.

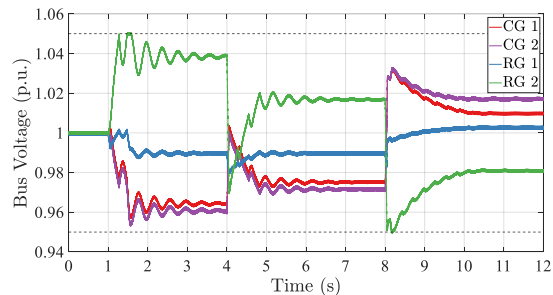


Fig. 14. Trajectories of bus voltages with $1000 \mu\text{s}$ communication delay.

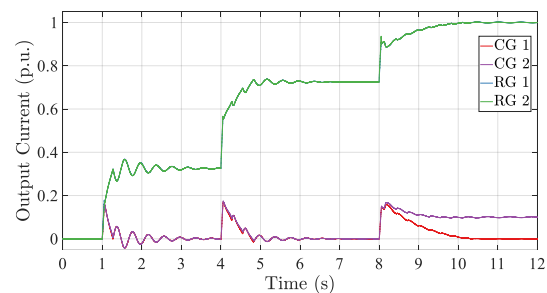


Fig. 15. Trajectories of output currents with $1000 \mu\text{s}$ communication delay.

VI. CONCLUSION

In this article, a distributed discrete-time optimal control algorithm is developed, in which the generation cost of CGs is minimized and the energy utilization of RGs is maximized. A certain degree of proportional load sharing among the RGs is also achieved. With the designed control algorithm, the bus voltages can be maintained in their safe operating ranges. The stability and convergence of the proposed algorithm are

analyzed through Lyapunov synthesis. The bus voltages and output currents are proved to converge to their optimal operating points asymptotically. Finally, the advantages of the developed control algorithm with constant and dynamic RG capacities, line parameter uncertainties, and communication delays are illustrated by switch-level dc microgrid simulations.

In the future, theoretical stability analyses with communication delays and parameter uncertainties will be further investigated. Besides, the interactions between the optimal controller and the local control loops will be analyzed.

APPENDIX: PROOF OF THEOREM 1

To facilitate the analysis, rewriting (8)-(10) in a compact form yields

$$\mathbf{V}_{k+1} = \mathbf{P}_{\Omega_V}[\mathbf{V}_k + \alpha \mathbf{G}(\mathbf{y}_k + \hat{\mathbf{I}}_k - \mathbf{I}_k)] \quad (11)$$

$$\hat{\mathbf{I}}_{k+1} = \mathbf{P}_{\Omega_I}[\hat{\mathbf{I}}_k - \alpha(\boldsymbol{\mu}_k + \mathbf{y}_k + \hat{\mathbf{I}}_k - \mathbf{I}_k)] \quad (12)$$

$$\mathbf{y}_k = \mathbf{y}_{k-1} + \hat{\mathbf{I}}_k - \mathbf{I}_k \quad (13)$$

where $\mathbf{V}_k = [V_{1k}, \dots, V_{nk}]^T \in \mathbb{R}^n$, $\hat{\mathbf{I}}_k = [\hat{I}_{1k}, \dots, \hat{I}_{nk}]^T \in \mathbb{R}^n$, $\mathbf{y}_k = [y_{1k}, \dots, y_{nk}]^T \in \mathbb{R}^n$, and $\boldsymbol{\mu}_k = [\mu_{1k}, \dots, \mu_{nk}]^T \in \mathbb{R}^n$.

The convergence and stability of the proposed controller are proved by the Lyapunov theory. Let $\mathbf{V}^*, \mathbf{I}^* \in \mathbb{R}^n$ be an optimal solution to the problem (6). Further, there exist $\mathbf{y}^* \in \mathbb{R}^n$ such that equations in (7) hold. Define the following functions: $W_1(\mathbf{V}_k) = \|\mathbf{V}_k - \mathbf{V}^*\|^2$, $W_2(\hat{\mathbf{I}}_k) = \|\hat{\mathbf{I}}_k - \mathbf{I}^*\|^2$, and $W_3(\mathbf{y}_k) = \|\mathbf{y}_k - \mathbf{y}^*\|^2$. Subsequently, their differences are calculated separately.

1) Denote $\mathbf{P}_{\Omega_V k} = \mathbf{P}_{\Omega_V}[\mathbf{V}_k + \alpha \mathbf{G}(\mathbf{y}_k + \hat{\mathbf{I}}_k - \mathbf{I}_k)]$ which follows that $\mathbf{V}_{k+1} = \mathbf{P}_{\Omega_V k}$. Then the difference of W_1 is

$$\begin{aligned} W_1(\mathbf{V}_{k+1}) - W_1(\mathbf{V}_k) &= \|\mathbf{V}_{k+1} - \mathbf{V}^*\|^2 - \|\mathbf{V}_k - \mathbf{V}^*\|^2 \\ &= \|\mathbf{P}_{\Omega_V k} - \mathbf{V}^*\|^2 - \|\mathbf{V}_k - \mathbf{V}^*\|^2 \\ &= (\mathbf{P}_{\Omega_V k} - \mathbf{V}_k)^T (\mathbf{P}_{\Omega_V k} + \mathbf{V}_k - 2\mathbf{V}^*) \\ &= -\|\mathbf{P}_{\Omega_V k} - \mathbf{V}_k\|^2 + 2(\mathbf{P}_{\Omega_V k} - \mathbf{V}_k)^T (\mathbf{P}_{\Omega_V k} - \mathbf{V}^*) \\ &= -\|\mathbf{P}_{\Omega_V k} - \mathbf{V}_k\|^2 + 2[\mathbf{P}_{\Omega_V k} - \mathbf{V}_k - \alpha \mathbf{G}(\mathbf{y}_k + \hat{\mathbf{I}}_k - \mathbf{I}_k)]^T (\mathbf{P}_{\Omega_V k} - \mathbf{V}^*) + 2\alpha \mathbf{G}(\mathbf{y}_k + \hat{\mathbf{I}}_k - \mathbf{I}_k)^T \\ &\quad \times (\mathbf{P}_{\Omega_V k} - \mathbf{V}^*). \end{aligned}$$

Let $\mathbf{u} = \mathbf{V}_k + \alpha \mathbf{G}(\mathbf{y}_k + \hat{\mathbf{I}}_k - \mathbf{I}_k)$ and $\mathbf{v} = \mathbf{V}^*$, from the inequality in Lemma 1, there is $[\mathbf{P}_{\Omega_V k} - \mathbf{V}_k - \alpha \mathbf{G}(\mathbf{y}_k + \hat{\mathbf{I}}_k - \mathbf{I}_k)]^T (\mathbf{P}_{\Omega_V k} - \mathbf{V}^*) \leq 0$. Then combining with $\mathbf{V}_{k+1} = \mathbf{P}_{\Omega_V k}$ gives

$$W_1(\mathbf{V}_{k+1}) - W_1(\mathbf{V}_k) \leq -\|\mathbf{V}_{k+1} - \mathbf{V}_k\|^2 + 2\alpha(\mathbf{V}_{k+1} - \mathbf{V}^*)^T \mathbf{G}(\mathbf{y}_k + \hat{\mathbf{I}}_k - \mathbf{I}_k). \quad (14)$$

According to (7) and Lemma 1, the following inequality holds $(\mathbf{V}^* - \mathbf{V}_{k+1})^T \mathbf{G}\mathbf{y}^* \geq 0$.

Then (14) becomes

$$W_1(\mathbf{V}_{k+1}) - W_1(\mathbf{V}_k) \leq -\|\mathbf{V}_{k+1} - \mathbf{V}_k\|^2 + 2\alpha(\mathbf{V}_{k+1} - \mathbf{V}^*)^T \mathbf{G}(\mathbf{y}_k - \mathbf{y}^* + \hat{\mathbf{I}}_k - \mathbf{I}_k). \quad (15)$$

Considering $\mathbf{G}\mathbf{V}^* = \mathbf{I}^* - \mathbf{I}_L$, $\mathbf{G}\mathbf{V}_{k+1} = \mathbf{I}_{k+1} - \mathbf{I}_L$, then (15) becomes

$$W_1(\mathbf{V}_{k+1}) - W_1(\mathbf{V}_k) \leq -\|\mathbf{V}_{k+1} - \mathbf{V}_k\|^2 + 2\alpha(\mathbf{I}_{k+1} - \mathbf{I}^*)^T (\mathbf{y}_k - \mathbf{y}^* + \hat{\mathbf{I}}_k - \mathbf{I}_k). \quad (16)$$

2) Denote $\mathbf{P}_{\Omega_I k} = \mathbf{P}_{\Omega_I}[\hat{\mathbf{I}}_k - \alpha(\boldsymbol{\mu}_k + \mathbf{y}_k + \hat{\mathbf{I}}_k - \mathbf{I}_k)]$ which follows that $\hat{\mathbf{I}}_{k+1} = \mathbf{P}_{\Omega_I k}$. Then one has

$$W_2(\hat{\mathbf{I}}_{k+1}) - W_2(\hat{\mathbf{I}}_k) = \|\hat{\mathbf{I}}_{k+1} - \mathbf{I}^*\|^2 - \|\hat{\mathbf{I}}_k - \mathbf{I}^*\|^2$$

$$\begin{aligned} &= \|\mathbf{P}_{\Omega_I k} - \mathbf{I}^*\|^2 - \|\hat{\mathbf{I}}_k - \mathbf{I}^*\|^2 \\ &= (\mathbf{P}_{\Omega_I k} - \hat{\mathbf{I}}_k)^T (\mathbf{P}_{\Omega_I k} + \hat{\mathbf{I}}_k - 2\mathbf{I}^*) \\ &= -\|\mathbf{P}_{\Omega_I k} - \hat{\mathbf{I}}_k\|^2 + 2(\mathbf{P}_{\Omega_I k} - \hat{\mathbf{I}}_k)^T (\mathbf{P}_{\Omega_I k} - \mathbf{I}^*) \\ &= -\|\mathbf{P}_{\Omega_I k} - \hat{\mathbf{I}}_k\|^2 + 2[\mathbf{P}_{\Omega_I k} - \hat{\mathbf{I}}_k + \alpha(\boldsymbol{\mu}_k + \mathbf{y}_k + \hat{\mathbf{I}}_k - \mathbf{I}_k)]^T (\mathbf{P}_{\Omega_I k} - \mathbf{I}^*) - 2\alpha(\boldsymbol{\mu}_k + \mathbf{y}_k + \hat{\mathbf{I}}_k - \mathbf{I}_k)^T \\ &\quad \times (\mathbf{P}_{\Omega_I k} - \mathbf{I}^*). \end{aligned}$$

Let $\mathbf{u} = \hat{\mathbf{I}}_k - \alpha(\boldsymbol{\mu}_k + \mathbf{y}_k + \hat{\mathbf{I}}_k - \mathbf{I}_k)$ and $\mathbf{v} = \mathbf{I}^*$, from the inequality in Lemma 1, there is $[\mathbf{P}_{\Omega_I k} - \hat{\mathbf{I}}_k + \alpha(\boldsymbol{\mu}_k + \mathbf{y}_k + \hat{\mathbf{I}}_k - \mathbf{I}_k)]^T (\mathbf{P}_{\Omega_I k} - \mathbf{I}^*) \leq 0$. Then combining with $\hat{\mathbf{I}}_{k+1} = \mathbf{P}_{\Omega_I k}$ gives

$$\begin{aligned} W_2(\hat{\mathbf{I}}_{k+1}) - W_2(\hat{\mathbf{I}}_k) &\leq -\|\hat{\mathbf{I}}_{k+1} - \hat{\mathbf{I}}_k\|^2 \\ &\quad - 2\alpha(\hat{\mathbf{I}}_{k+1} - \mathbf{I}^*)^T (\mathbf{y}_k + \hat{\mathbf{I}}_k - \mathbf{I}_k) \\ &\quad - 2\alpha(\hat{\mathbf{I}}_{k+1} - \mathbf{I}^*)^T \boldsymbol{\mu}_k. \end{aligned} \quad (17)$$

From the convexity of f , it has $(\hat{\mathbf{I}}_k - \mathbf{I}^*)^T \boldsymbol{\mu}_k \geq f(\hat{\mathbf{I}}_k) - f(\mathbf{I}^*)$ and $(\hat{\mathbf{I}}_{k+1} - \hat{\mathbf{I}}_k)^T \boldsymbol{\mu}_{k+1} \geq f(\hat{\mathbf{I}}_{k+1}) - f(\hat{\mathbf{I}}_k)$, then

$$\begin{aligned} (\hat{\mathbf{I}}_{k+1} - \mathbf{I}^*)^T \boldsymbol{\mu}_k &= (\hat{\mathbf{I}}_{k+1} - \hat{\mathbf{I}}_k)^T \boldsymbol{\mu}_k + (\hat{\mathbf{I}}_k - \mathbf{I}^*)^T \boldsymbol{\mu}_k \\ &\geq (\hat{\mathbf{I}}_{k+1} - \hat{\mathbf{I}}_k)^T \boldsymbol{\mu}_k + f(\hat{\mathbf{I}}_k) - f(\mathbf{I}^*) \\ &= (\hat{\mathbf{I}}_{k+1} - \hat{\mathbf{I}}_k)^T (\boldsymbol{\mu}_k - \boldsymbol{\mu}_{k+1}) \\ &\quad + (\hat{\mathbf{I}}_{k+1} - \hat{\mathbf{I}}_k)^T \boldsymbol{\mu}_{k+1} + f(\hat{\mathbf{I}}_k) - f(\mathbf{I}^*) \\ &\geq (\hat{\mathbf{I}}_{k+1} - \hat{\mathbf{I}}_k)^T (\boldsymbol{\mu}_k - \boldsymbol{\mu}_{k+1}) + f(\hat{\mathbf{I}}_{k+1}) - f(\mathbf{I}^*) \end{aligned}$$

Combining it with (17) gives

$$\begin{aligned} W_2(\hat{\mathbf{I}}_{k+1}) - W_2(\hat{\mathbf{I}}_k) &\leq -\|\hat{\mathbf{I}}_{k+1} - \hat{\mathbf{I}}_k\|^2 \\ &\quad - 2\alpha(\hat{\mathbf{I}}_{k+1} - \mathbf{I}^*)^T (\mathbf{y}_k + \hat{\mathbf{I}}_k - \mathbf{I}_k) \\ &\quad + 2\alpha(\hat{\mathbf{I}}_{k+1} - \hat{\mathbf{I}}_k)^T (\boldsymbol{\mu}_{k+1} - \boldsymbol{\mu}_k) \\ &\quad - 2\alpha[f(\hat{\mathbf{I}}_{k+1}) - f(\mathbf{I}^*)]. \end{aligned} \quad (18)$$

According to (7) and Lemma 1, the following inequality holds

$$(\hat{\mathbf{I}}_{k+1} - \mathbf{I}^*)^T (\boldsymbol{\mu}^* + \mathbf{y}^*) \geq 0$$

From the convexity of f , one gets that $(\hat{\mathbf{I}}_{k+1} - \mathbf{I}^*)^T \boldsymbol{\mu}^* \leq f(\hat{\mathbf{I}}_{k+1}) - f(\mathbf{I}^*)$. Then, $f(\hat{\mathbf{I}}_{k+1}) - f(\mathbf{I}^*) \geq -(\hat{\mathbf{I}}_{k+1} - \mathbf{I}^*)^T \mathbf{y}^*$ and combining with (18) follows that

$$\begin{aligned} W_2(\hat{\mathbf{I}}_{k+1}) - W_2(\hat{\mathbf{I}}_k) &\leq -\|\hat{\mathbf{I}}_{k+1} - \hat{\mathbf{I}}_k\|^2 \\ &\quad - 2\alpha(\hat{\mathbf{I}}_{k+1} - \mathbf{I}^*)^T (\mathbf{y}_k - \mathbf{y}^* + \hat{\mathbf{I}}_k - \mathbf{I}_k) \\ &\quad + 2\alpha(\hat{\mathbf{I}}_{k+1} - \hat{\mathbf{I}}_k)^T (\boldsymbol{\mu}_{k+1} - \boldsymbol{\mu}_k). \end{aligned} \quad (19)$$

3) Since $\mathbf{y}_k = \mathbf{y}_{k-1} + \hat{\mathbf{I}}_k - \mathbf{I}_k$, there is $\mathbf{y}_{k+1} = \mathbf{y}_k + \hat{\mathbf{I}}_{k+1} - \mathbf{I}_{k+1}$. Therefore, the difference of W_3 is

$$\begin{aligned} W_3(\mathbf{y}_{k+1}) - W_3(\mathbf{y}_k) &= \|\mathbf{y}_{k+1} - \mathbf{y}^*\|^2 - \|\mathbf{y}_k - \mathbf{y}^*\|^2 \\ &= \|\mathbf{y}_k - \mathbf{y}^* + \hat{\mathbf{I}}_{k+1} - \mathbf{I}_{k+1}\|^2 - \|\mathbf{y}_k - \mathbf{y}^*\|^2 \\ &= (\hat{\mathbf{I}}_{k+1} - \mathbf{I}_{k+1})^T [2(\mathbf{y}_k - \mathbf{y}^*) + \hat{\mathbf{I}}_{k+1} - \mathbf{I}_{k+1}] \\ &= 2(\hat{\mathbf{I}}_{k+1} - \mathbf{I}_{k+1})^T (\mathbf{y}_k - \mathbf{y}^*) \\ &\quad + \|\hat{\mathbf{I}}_{k+1} - \mathbf{I}_{k+1} - (\hat{\mathbf{I}}_k - \mathbf{I}_k)\|^2 \\ &\quad + 2(\hat{\mathbf{I}}_{k+1} - \mathbf{I}_{k+1})^T (\hat{\mathbf{I}}_k - \mathbf{I}_k) - \|\hat{\mathbf{I}}_k - \mathbf{I}_k\|^2 \\ &= 2(\hat{\mathbf{I}}_{k+1} - \mathbf{I}_{k+1})^T (\mathbf{y}_k - \mathbf{y}^* + \hat{\mathbf{I}}_k - \mathbf{I}_k) \\ &\quad + \|\hat{\mathbf{I}}_{k+1} - \mathbf{I}_{k+1} - (\hat{\mathbf{I}}_k - \mathbf{I}_k)\|^2 - \|\hat{\mathbf{I}}_k - \mathbf{I}_k\|^2. \end{aligned}$$

Now, consider the following Lyapunov function candidate as

$$W(\mathbf{V}_k, \hat{\mathbf{I}}_k, \mathbf{y}_k) = W_1(\mathbf{V}_k) + W_2(\hat{\mathbf{I}}_k) + \alpha W_3(\mathbf{y}_k).$$

Based on (16), (19), and the difference of W_3 , one has

$$\begin{aligned}
 W(\mathbf{V}_{k+1}, \hat{\mathbf{I}}_{k+1}, \mathbf{y}_{k+1}) - W(\mathbf{V}_k, \hat{\mathbf{I}}_k, \mathbf{y}_k) \\
 \leq -\|\mathbf{V}_{k+1} - \mathbf{V}_k\|^2 - \|\hat{\mathbf{I}}_{k+1} - \hat{\mathbf{I}}_k\|^2 \\
 + 2\alpha(\hat{\mathbf{I}}_{k+1} - \hat{\mathbf{I}}_k)^T(\boldsymbol{\mu}_{k+1} - \boldsymbol{\mu}_k) \\
 + \alpha\|\hat{\mathbf{I}}_{k+1} - \mathbf{I}_{k+1} - (\hat{\mathbf{I}}_k - \mathbf{I}_k)\|^2 \\
 - \alpha\|\hat{\mathbf{I}}_k - \mathbf{I}_k\|^2.
 \end{aligned} \quad (20)$$

Considering that $\sigma \geq 2 \max_i a_i$, one has

$$(\hat{\mathbf{I}}_{k+1} - \hat{\mathbf{I}}_k)^T(\boldsymbol{\mu}_{k+1} - \boldsymbol{\mu}_k) \leq \sigma\|\hat{\mathbf{I}}_{k+1} - \hat{\mathbf{I}}_k\|^2.$$

Further, according to (2), one has

$$\begin{aligned}
 \|\hat{\mathbf{I}}_{k+1} - \mathbf{I}_{k+1} - (\hat{\mathbf{I}}_k - \mathbf{I}_k)\|^2 &= \|\hat{\mathbf{I}}_{k+1} - \hat{\mathbf{I}}_k - \mathbf{G}(\mathbf{V}_{k+1} - \mathbf{V}_k)\|^2 \\
 &\leq \|\hat{\mathbf{I}}_{k+1} - \hat{\mathbf{I}}_k\|^2 + \|\mathbf{G}(\mathbf{V}_{k+1} - \mathbf{V}_k)\|^2 \\
 &\quad - 2(\hat{\mathbf{I}}_{k+1} - \hat{\mathbf{I}}_k)^T \mathbf{G}(\mathbf{V}_{k+1} - \mathbf{V}_k).
 \end{aligned}$$

Thereafter, (20) becomes

$$\begin{aligned}
 W(\mathbf{V}_{k+1}, \hat{\mathbf{I}}_{k+1}, \mathbf{y}_{k+1}) - W(\mathbf{V}_k, \hat{\mathbf{I}}_k, \mathbf{y}_k) \\
 \leq -(\mathbf{x}_{k+1} - \mathbf{x}_k)^T(\mathbb{I}_{2n} - \alpha\mathbf{H})(\mathbf{x}_{k+1} - \mathbf{x}_k) \\
 - \alpha\|\hat{\mathbf{I}}_k - \mathbf{I}_k\|^2.
 \end{aligned}$$

with $\mathbb{I}_{2n} \in \mathbb{R}^{2n \times 2n}$ being the identity matrix and $\mathbf{x}_k = [\mathbf{V}_k^T, \hat{\mathbf{I}}_k^T]^T \in \mathbb{R}^{2n}$. Since $\alpha \leq 1/\lambda_{\max}(\mathbf{H})$, the matrix $\mathbb{I}_{2n} - \alpha\mathbf{H}$ is positive definite. Then the difference of W is negative definite.

According to LaSalle's invariance principle for discrete-time systems [26], one has

$$\lim_{k \rightarrow \infty} \mathbf{V}_k = \tilde{\mathbf{V}}, \lim_{k \rightarrow \infty} \mathbf{I}_k = \tilde{\mathbf{I}}, \lim_{k \rightarrow \infty} \hat{\mathbf{I}}_k = \tilde{\mathbf{I}}$$

with $\tilde{\mathbf{V}} \in \mathbb{R}^n$, $\tilde{\mathbf{I}} \in \mathbb{R}^n$, $\tilde{\mathbf{y}} \in \mathbb{R}^n$ satisfying

$$\begin{cases}
 \tilde{\mathbf{V}} - \mathbf{P}_{\Omega_V}(\tilde{\mathbf{V}} + \alpha\mathbf{G}\tilde{\mathbf{y}}) = \mathbf{0} \\
 \tilde{\mathbf{I}} - \mathbf{P}_{\Omega_I}[\tilde{\mathbf{I}} - \alpha(\tilde{\boldsymbol{\mu}} + \tilde{\mathbf{y}})] = \mathbf{0} \\
 \tilde{\mathbf{I}} - \mathbf{G}\tilde{\mathbf{V}} - \mathbf{I}_L = \mathbf{0}
 \end{cases}$$

where $\tilde{\boldsymbol{\mu}} = [\tilde{\mu}_1, \tilde{\mu}_2, \dots, \tilde{\mu}_n]^T \in \mathbb{R}^n$ with

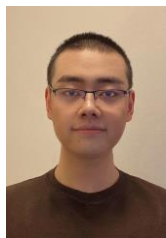
$$\tilde{\mu}_i = \left. \frac{\partial f_i}{\partial I_i} \right|_{I_i = \tilde{I}_i} = 2a_i \tilde{I}_i + b_i, i \in \mathcal{V}_E.$$

Hence, $\tilde{\mathbf{V}}$ and $\tilde{\mathbf{I}}$ is an optimal solution of (6) since it satisfies the optimal condition in (7). Thus, \mathbf{V}_k and \mathbf{I}_k will converge to an optimal solution to the optimization problem (6). The proof is complete.

REFERENCES

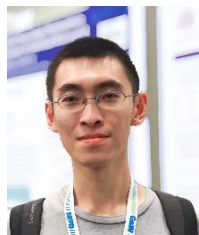
- [1] L. Xing, F. Guo, X. Liu, C. Wen, Y. Mishra, and Y. C. Tian, "Voltage restoration and adjustable current sharing for DC microgrid with time delay via distributed secondary control," *IEEE Trans. Sustain. Energy*, vol. 12, no. 2, pp. 1068–1077, 2021.
- [2] B. Wang, M. Sechilariu, and F. Locment, "Intelligent DC microgrid with smart grid communications: Control strategy consideration and design," *IEEE Trans. Smart Grid*, vol. 3, no. 4, pp. 2148–2156, 2012.
- [3] Y. Xu, W. Zhang, W. Liu, X. Wang, F. Ferrese, C. Zang, and H. Yu, "Distributed subgradient-based coordination of multiple renewable generators in a microgrid," *IEEE Trans. Power Syst.*, vol. 29, no. 1, pp. 23–33, 2013.
- [4] W. Zhang, Y. Xu, W. Liu, F. Ferrese, and L. Liu, "Fully distributed coordination of multiple DFIGs in a microgrid for load sharing," *IEEE Trans. Smart Grid*, vol. 4, no. 2, pp. 806–815, 2013.
- [5] S. Wang, M. Du, L. Lu, W. Xing, K. Sun, and M. Ouyang, "Multilevel energy management of a DC microgrid based on virtual-battery model considering voltage regulation and economic optimization," *IEEE J. Emerg. Sel. Topics Power Electron.*, vol. 9, no. 3, pp. 2881–2895, 2021.
- [6] Y. Chen, Z. Zhang, H. Chen, and H. Zheng, "Robust UC model based on multi-band uncertainty set considering the temporal correlation of wind/load prediction errors," *IET Gener. Transmiss. Distrib.*, vol. 14, no. 2, pp. 180–190, 2019.
- [7] Y. Chen, Z. Zhang, Z. Liu, P. Zhang, Q. Ding, X. Liu, and W. Wang, "Robust N-k CCUC model considering the fault outage probability of

- units and transmission lines," *IET Gener. Transmiss. Distrib.*, vol. 13, no. 17, pp. 3782–3791, 2019.
- [8] W. Zhang, Y. Xu, W. Liu, C. Zang, and H. Yu, "Distributed online optimal energy management for smart grids," *IEEE Trans. Ind. Informat.*, vol. 11, no. 3, pp. 717–727, 2015.
- [9] N. Rahbari-Asr, Y. Zhang, and M.-Y. Chow, "Consensus-based distributed scheduling for cooperative operation of distributed energy resources and storage devices in smart grids," *IET Gener., Transmiss. Distrib.*, vol. 10, no. 5, pp. 1268–1277, 2016.
- [10] A. Garcés, "Convex optimization for the optimal power flow on DC distribution systems," in *Handbook Optim. Elect. Power Distrib. Syst.* Springer, 2020, pp. 121–137.
- [11] A. Bracale, P. Caramia, G. Carpinelli, E. Mancini, and F. Mottola, "Optimal control strategy of a DC micro grid," *Int. J. Elect. Power Energy Syst.*, vol. 67, pp. 25–38, 2015.
- [12] S. Moayedi and A. Davoudi, "Unifying distributed dynamic optimization and control of islanded DC microgrids," *IEEE Trans. Power Electron.*, vol. 32, no. 3, pp. 2329–2346, 2016.
- [13] Z. Wang, W. Wu, and B. Zhang, "A distributed control method with minimum generation cost for DC microgrids," *IEEE Trans. Energy Convers.*, vol. 31, no. 4, pp. 1462–1470, 2016.
- [14] Z. Wang, F. Liu, Y. Chen, S. H. Low, and S. Mei, "Unified distributed control of stand-alone DC microgrids," *IEEE Trans. Smart Grid*, vol. 10, no. 1, pp. 1013–1024, 2017.
- [15] Z. Fan, B. Fan, J. Peng, and W. Liu, "Operation loss minimization targeted distributed optimal control of DC microgrids," *IEEE Syst. J.*, to be published, doi: 10.1109/JSYST.2020.3035059.
- [16] J. Peng, B. Fan, and W. Liu, "Voltage-based distributed optimal control for generation cost minimization and bounded bus voltage regulation in DC microgrids," *IEEE Trans. Smart Grid*, vol. 12, no. 1, pp. 106–116, 2021.
- [17] B. Fan, J. Peng, Q. Yang, and W. Liu, "Distributed periodic event-triggered algorithm for current sharing and voltage regulation in DC microgrids," *IEEE Trans. Smart Grid*, vol. 11, no. 1, pp. 577–589, 2019.
- [18] B. Fan, S. Guo, J. Peng, Q. Yang, W. Liu, and L. Liu, "A consensus-based algorithm for power sharing and voltage regulation in DC microgrids," *IEEE Trans. Ind. Informat.*, vol. 16, no. 6, pp. 3987–3996, 2019.
- [19] L. Meng, T. Dragicevic, J. Roldán-Pérez, J. C. Vasquez, and J. M. Guerrero, "Modeling and sensitivity study of consensus algorithm-based distributed hierarchical control for DC microgrids," *IEEE Trans. Smart Grid*, vol. 7, no. 3, pp. 1504–1515, 2015.
- [20] D. Nešić and L. Grüne, "Lyapunov-based continuous-time nonlinear controller redesign for sampled-data implementation," *Automatica*, vol. 41, no. 7, pp. 1143–1156, 2005.
- [21] B. Fan, Q. Yang, S. Jagannathan, and Y. Sun, "Output-constrained control of nonlinear multiagent systems with partially unknown control directions," *IEEE Trans. Autom. Control*, vol. 64, no. 9, pp. 3936–3942, 2019.
- [22] M. Andreasson, R. Wiget, D. V. Dimarogonas, K. H. Johansson, and G. Andersson, "Distributed frequency control through MTDC transmission systems," *IEEE Trans. Power Syst.*, vol. 32, no. 1, pp. 250–260, 2017.
- [23] D. Kinderlehrer and G. Stampacchia, *An introduction to variational inequalities and their applications*, Philadelphia, PA, USA, 2000.
- [24] Q. Liu, S. Yang, and Y. Hong, "Constrained consensus algorithms with fixed step size for distributed convex optimization over multiagent networks," *IEEE Trans. Autom. Control*, vol. 62, no. 8, pp. 4259–4265, 2017.
- [25] D. Xu, Y. Dai, C. Yang, and X. Yan, "Adaptive fuzzy sliding mode command-filtered backstepping control for islanded PV microgrid with energy storage system," *J. Franklin Inst.*, vol. 356, no. 4, pp. 1880–1898, 2019.
- [26] J. P. LaSalle, *The stability and control of discrete processes*, New York, NY, USA, 2012, vol. 62.



Zhen Fan (Graduate Student Member, IEEE) received the B.S. degree in electrical engineering from the North China Electric Power University, Baoding, Hebei, China, in 2017 and the M.S. degree in electrical engineering from Lehigh University, Bethlehem, PA, USA. He is currently pursuing the Ph.D. degree in electrical engineering at Lehigh University.

His research interests include microgrid, distributed control, renewable energy systems, and power system.



Bo Fan (Member, IEEE) received the B.S. degree in automation and Ph.D. degree in control science and engineering from Zhejiang University, Hangzhou, China, in 2014 and 2019, respectively.

Since 2020, he has been with the Department of Energy Technology, Aalborg University, Aalborg, Denmark, where he is currently a Postdoctoral Researcher. His research interests include distributed control, nonlinear systems, smart grid, and renewable energy systems.

Dr. Fan was the recipient of the 2019 Outstanding Reviewer Award of IEEE TRANSACTIONS ON POWER SYSTEMS, the 2019 Best Reviewer Award of IEEE TRANSACTIONS ON SMART GRID, and the Marie Skłodowska-Curie Individual Fellowship in 2021.



Wei Zhang (Senior Member, IEEE) received the B.S. and M.S. degrees in electrical engineering from the Harbin Institute of Technology, Harbin, China, in 2007 and 2009, respectively, and the Ph.D. degree in electrical and computer engineering from the New Mexico State University, Las Cruces, NM, USA, in 2013.

He was an Associate Professor with the School of Electrical Engineering and Its Automation, Harbin Institute of Technology, Harbin, China, from 2014 to 2019, and a Postdoctoral Researcher with the University of Central Florida, Orlando, FL, USA, from 2019 to 2021. He is currently a Postdoctoral Researcher with the Department of Electrical and Computer Engineering, Lehigh University, Bethlehem, PA, USA. His research interests include distributed control and optimization, microgrids control and optimization, and machine learning in power system applications.



Wenxin Liu (Senior Member, IEEE) received the B.S. degree in industrial automation and the M.S. degree in control theory and applications from Northeastern University, Shenyang, China, in 1996 and 2000, respectively, and the Ph.D. degree in electrical engineering from the Missouri University of Science and Technology (formerly University of Missouri–Rolla),

Rolla, MO, USA, in 2005.

From 2005 to 2009, he was an Assistant Scholar Scientist with the Center for Advanced Power Systems, Florida State University, Tallahassee, FL, USA. From 2009 to 2014, he was an Assistant Professor with the Klipsch School of Electrical and Computer Engineering, New Mexico State University, Las Cruces, NM, USA. He is currently an Associate Professor with the Department of Electrical and Computer Engineering, Lehigh University, Bethlehem, PA, USA. His research interests include power systems, power electronics, and controls.

Dr. Liu is an Editor of the IEEE TRANSACTIONS ON SMART GRID, the IEEE TRANSACTIONS ON POWER SYSTEMS, and the Journal of Electrical Engineering & Technology, and an Associate Editor of the IEEE TRANSACTIONS ON INDUSTRIAL INFORMATICS.